A Voltage Controlled Overcurrent-based Adaptive Protection Scheme for Microgrids

Aadityaa Padmanabhan*, Tapas Kumar Barik*, Sean McGuinness**, Mobolaji Bello*
*Electric Power Research Institute, Knoxville, USA
**EPRI Europe DAC, Dublin, Ireland

Amin Zamani, Mehrdad Sheikholeslami
Quanta Technology, LLC
USA

Abstract—**Modern distribution feeders can facilitate and enable microgrid operation. In such cases, the protection systems need to meet the key requirements, such as reliability and sensitivity, under both grid-connected and islanded operating modes. Replacement of existing protection assets to enable safe, secure, and dependable microgrid protection can incur significant costs which, in turn, makes some microgrids cost prohibitive. This paper presents a cost-effective adaptive protection scheme using commonly used voltage-controlled overcurrent elements which can be retrofitted to existing electronic reclosers. The scheme can be implemented without any communication link to the microgrid controller. Hardware in the Loop (HIL) testing was used to evaluate the performance of the scheme for a real-case microgrid under various test scenarios. The test results showcase the improved efficacy of the adaptive logic for higher DER penetration levels.**

Index Terms—**Voltage-controlled overcurrent protection, DER, Hardware-in-the-loop, RTDS.**

I. Introduction

Design and testing of microgrid protection solutions can be a resource-intensive effort. Where existing distribution feeders are converted to enable microgrid operation, the protection systems need to meet reliability and sensitivity requirements under both grid-connected and island operating modes. When a microgrid transitions from grid-connected mode to island mode, the short-circuit current source changes from the grid to the Distributed Energy Resources (DERs) used to supply the islanded microgrid. Most radial distribution grids are protected by non-directional overcurrent protective devices, assuming unidirectional short circuit currents. If a DER is located at the opposite end of the feeder to the grid-connection point, it can cause mis-coordination of protective devices. The short circuit levels can also dramatically reduce between grid-connected and islanded modes as DER are typically much weaker short circuit current sources. The impact of such DER on general protection schemes of power distribution systems ([1]-[4]) as well as microgrid protection has been studied in the past ([5]-[9]). Distribution feeder protection is coordinated assuming a certain minimum fault current level. Thus, protection sensitivity may need to be lowered significantly when operating in island mode.

Where possible, it is preferred to design microgrid protection systems such that they can adequately protect the feeder in both grid-connected and islanded modes without changing settings or enabling/disabling functions; this will avoid the need for modifying protection and simplify the overall design. However, it may not always be practical to use a single group of settings. This is due to the change in the short circuit current direction, difference in short circuit current magnitudes, and negative sequence current characteristics between grid-connected and islanded modes. The overcurrent settings and functions may thus be required to adapt to keep the reclosers coordinated.

Replacement of existing protection assets to enable safe, secure, and dependable microgrid protection can incur significant costs. This paper presents a cost-effective adaptive protection scheme which can be easily implemented in existing electronic reclosers. The proposed logic aims to protect the microgrid under different operating modes, and transitions between operating modes, as well as in cases with component and communications failures. The scheme is based on a voltage-controlled overcurrent protection algorithm, which can be implemented either using logic that releases or blocks operation based on the microgrid state or using relay settings groups. The scheme is intended to protect microgrids irrespective of the type or size of their energy resources; this includes microgrids that are supplied by synchronous generators, those entirely sourced by inverter-based resources (IBR) such as battery energy storage systems (BESS), and/or hybrid microgrids with a combination of both synchronous generators and IBRs. The scheme can be implemented with or without communications to a microgrid controller and has the logic to fall into a fail-safe operating mode if it is unable to determine the microgrid operating state. The protection settings and scheme evaluation were performed using widely used commercial short circuit analysis tools.

When the microgrid transitions to the islanded mode, the main short circuit current sources change from the grid to the DER(s). Thus, the short circuit levels dramatically reduce between grid-connected and islanded modes due to the size and fault current capability of DERs. The existing protection relays were coordinated assuming there would be a much stronger source of fault current (grid-connected mode). Therefore, to maintain sensitivity and selectivity of the protection system, the protection design usually needs to be revised. The proposed scheme was implemented in a commercial, off-the-shelf protection relay and tested using a Hardware-in-the-Loop (HIL) testbed environment. Test scenarios included protection performance in grid-connected mode, islanded mode, during large motor starting events, and transformer energization. The scheme was found to meet all performance requirements.

The rest of the paper is structured as follows: Section II provides a brief background on microgrids and their different operating modes. Section III discusses the proposed adaptive protection design overview. Section IV outlines the various considerations and scenarios considered for the pre-deployment testing phase of the adaptive protection scheme. Section V presents the various test results that were carried out using HIL Real-Time Digital Simulator (RTDS) testing. Finally, the conclusions and ongoing as well as future work are summarized in Section VI.

II. Microgrid Background

Depending on their application and use cases, microgrids can operate under different conditions. There are several different microgrid phases or modes [10],[11]:

- *Grid connected and normal*: In this state, a microgrid remains connected to the main grid. The microgrid performs two main functions in this state: 1) coordinates the DER within the microgrid to provide grid-supportive services and 2) optimizes the overall performance of the microgrid by economically dispatching DER. In this mode, protection devices within the microgrid use their grid-connected configuration.

- *Grid connected and parallel (preparing to island):* Maintenance, repairs, and upgrades to existing transmission and distribution lines are common. This can result in sections of the grid being isolated and operated as a microgrid in islanded mode without being connected to the main grid. Adaptive protection devices usually switch to their configuration for islanded mode under such conditions.

- *Transitioning to stable island:* During this state, a sequence of steps results in disconnecting the microgrid, regulating the voltage and frequency by DERs and switching from grid-following to grid-forming mode, and enabling secondary controls in the grid-forming DER if there is a voltage or frequency issue. Switched grounding transformers are usually connected in this period. Adaptive protection devices may also switch to their configuration for islanded mode in this case.

- *Islanded and normal:* In this state, the microgrid is islanded and continues stable operation. The voltage and frequency of the microgrid are regulated by the grid-forming DER.

- *Islanded and ready to reconnect:* When the grid supply returns, the microgrid can reconnect with the main grid and continue operations in the grid-connected and normal mode. During this state, the microgrid goes through a sequence of steps before finally resynchronizing with the main grid.

- *Microgrid offline:* Certain unforeseen incidents—for example, faults in a microgrid can result in a voltage or frequency collapse, resulting in a blackout. To resume operations, the microgrid should then go through a blackstart process. This involves sequentially bringing together DER, restoring loads in islanded mode, and then integrating the microgrid with the main grid.

III. Adaptive protection Design

A. Adaptive protection success criteria

While designing the scheme, it is imperative to define some important success merits to correctly identify key design aspects of the scheme. The success of the microgrid adaptive protection logic design can be evaluated by the following measures. These success merits were translated to specific simulations and laboratory tests to validate the scheme.

- A scheme which can be readily deployed to common protection and controller equipment already in use by distribution grid utilities.
- A design that detects and isolates all credible low impedance balanced and unbalanced faults during normal and abnormal grid configurations.
- Protection that does not incorrectly trip during soft or hard black starts.
- Protection that does not trip during transformer inrush in the absence of a fault.
- Protection that does not trip during block loading, motor-starting, or cold-load pickup.

B. Adaptive protection design overview

Based on preliminary analysis, a voltage-controlled overcurrent protection scheme was chosen as the primary feeder protection method during islanded mode of operation, while conventional inverse time overcurrent protection can continue to be used in grid-connected mode. The conventional inverse time overcurrent protection element can be permanently enabled if their minimum pickup values exceed the maximum available short circuit current level in islanded mode. In such cases, the conventional inverse time overcurrent protection cannot trip during island mode and there is no need to disable it.

A voltage-controlled overcurrent element consists of a sensitive overcurrent element that is only enabled if the corresponding voltage dips below a set threshold (e.g., 0.5pu). Faults in islanded microgrids tend to result in the voltage collapsing on the faulted phase on account of the weak source energizing the microgrid under islanded mode. With this approach, most faults can be distinguished from load current using the under-voltage element (ANSI code 27) to control (supervise) the overcurrent element (ANSI code 50/51). The undervoltage pickup setting should be selected based on short circuit analysis and a reasonable estimation of load drop-out characteristics. The overcurrent pickup can be set below the fault current limit (e.g., 70% of the current limit) and an undervoltage pickup can be set below the drop-out voltage of most of the load (e.g., 0.5pu). Figure 1 shows the logic diagram of a typical voltage-controlled time inverse overcurrent element.

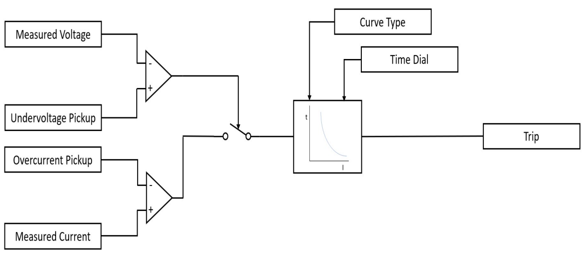

Figure 1. Typical Voltage controlled Overcurrent element logic diagram

The scheme can be de-centralized by dynamically blocking the voltage-controlled overcurrent element if the measured short circuit current exceeds a set threshold. The threshold is set such that it exceeds the maximum short circuit current magnitude which can occur while operating in island mode. Thus, if the measured current exceeds the threshold, the microgrid can only be in grid-connected mode. This scheme can be deployed on microgrids with multiple midline reclosers as the overcurrent curves can be time-graded to coordinate all the protection devices. If the microgrid includes DER at multiple locations and thus fault current could flow through a recloser in more than one direction, voltage-controlled directional overcurrent can be used.

Selection of the voltage-controlled overcurrent pickup current is based on available setting ranges, microgrid load characteristics (motor starting current, etc.), and minimum fault current levels (typically for medium or high impedance faults), while the time dial/delay is chosen based on downstream protection devices with which it must coordinate. Table I provides a summary of the proposed adaptive protection scheme.

TABLE I. DESCRIPTION OF PROTECTION UNDER MICROGRID OPERATING MODES

Operating Mode	Adaptive Protection description
Protection in Islanded Mode	Voltage-Controlled Overcurrent 50C/51C Example settings: • Undervoltage pickup 0.8pu • Overcurrent pickup equal to 50% of the maximum steady-state load current through recloser in islanded mode
Protection in Grid-Connected Mode	• Enable conventional inverse time overcurrent used if the measured current exceeds a set threshold. • Enable voltage-controlled overcurrent if the voltage sags and the current does not exceed a set threshold. • The threshold current is calculated as 120% of the maximum rms fundamental frequency short circuit current in islanded mode. • If the relay measures current greater than this value, then the microgrid must be grid-connected, so the voltage-controlled overcurrent element will be blocked.

The proposed logic can be deployed without the use of separate digital relay settings groups, but settings groups can be used, if preferred. The logic designs are supplemental; that is, they can be implemented alongside existing logic within the digital relay or controller. Appendix 1 documents the logic from Table I as it was programmed in the microprocessor relay for use in laboratory testing of the microgrid protection scheme.

IV. PRE-DEPLOYMENT TESTING

A. *Microgrid modeling in DIgSILENT PowerFactory*

To implement the proposed logic scheme for microgrids, the first task was to run preliminary Electromagnetic Transient (EMT) simulations on a simplified microgrid model. Operating scenarios of interest were identified, and corresponding simulations were performed to obtain three-phase voltage and current waveforms that could then be played back to the relay through a secondary injection three-phase test set so that the performance of the adaptive protection scheme can be observed, and its performance measured. Figure 2 illustrates the microgrid model that was created to test out the adaptive protection scheme based on the voltage-controlled overcurrent logic. The microgrid was modeled in DIgSILENT PowerFactory software to enable power flow, short-circuit, and time-domain EMT simulations to be performed. The microgrid model consists of a battery energy storage system (BESS), a BESS generator step-up transformer (BESS GSU), two feeder sections, multiple line reclosers, a load step-down transformer, and an induction motor (IM) as a dynamic load. The specifications of the various equipment are specified in Table II.

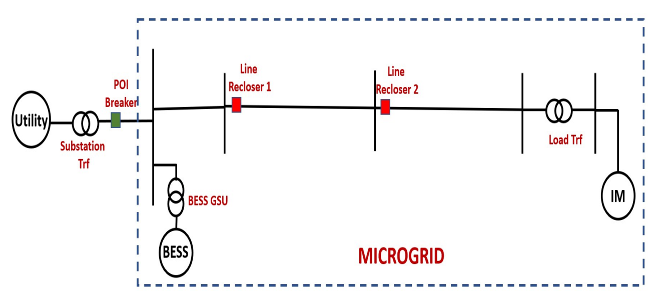

Figure 2. Layout of the Microgrid model

TABLE II. SPECIFICATIONS OF EQUIPMENT IN THE MICROGRID

Equipment Name	Nameplate Specifications
BESS	3MVA, 400V, 0.95 pf
BESS GSU	3.75MVA, 12.47/0.4kV Dyn0 %Z = 7, X/R = 20
Overall Feeder section	Length=4 mi, R1 = 0.016 ohm/mi, X1 = 0.16 ohm/mi, R0 = 0.048 ohm/mi, X0 = 0.48 ohm/mi
Load Transformers	0.5MVA – 3 MVA in size, 12.47/0.4kV Dyn0, %Z = 7, X/R = 20
Induction Motor	0.25-2.5 MW 0.4kV 0.82 pf

B. Test Scenarios

The adaptive protection logic proposed for microgrids needs to perform as expected for various positive and negative tests. The proposed adaptive protection scheme based on voltage-controlled overcurrent logic should come into effect once the Point of Interconnection (POI) breaker is open and the microgrid is in an islanded state. In the islanded state, the adaptive protection scheme should be able to correctly identify various balanced and unbalanced faults (both bolted and with resistance). It must be able to differentiate severe steady-state conditions such as load switching, motor starting, or transformer energization to ensure that the relays across the microgrid ride through these conditions. Keeping this in mind, the following scenarios were shortlisted for testing:

1. ***Islanded scenario:*** The utility main source is disconnected by tripping the POI breaker and the system inside the microgrid is at a steady state. The overall short circuit MVA level of the disconnected microgrid reduces.
2. ***Soft start scenario:*** The microgrid is in a black out condition, needing restoration; and the microgrid is energized by a blackstart process. The voltage profile of the microgrid system follows a ramp pattern with the help of the inverter controls associated with the BESS. This type of starting procedure usually avoids transformer inrush which might prove detrimental to the stability of the inverters. Gradually all the generation sources are brought up to their nominal steady state.
3. ***Hard start scenario:*** The microgrid generation sources are brought online first to their nominal steady state and then, their terminal buses are energized. Thereafter, the generator step-up LV/MV transformer is switched in, and finally the line reclosers in the network are closed sequentially. In case the loads have switches (such as in case of large induction motors), they can be switched on gradually one by one till the whole network is energized.
4. ***Motor start scenario:*** A huge dynamic load such as an induction motor might lead to severe voltage dips and hence might trick the protection logic to trip falsely for such unwarranted cases. The logic needs to ride through such scenarios and correctly distinguish these events from other fault conditions.
5. ***Transformer energization scenario*:** Similarly, transformer energization can cause high inrush currents in the network which might falsely lead to picking up the overcurrent element of the relays in the network. The adaptive protection scheme should also cater to these scenarios and must be able to correctly identify transformer inrush situations and not operate for this scenario.

C. Test Plan

Based on the test scenarios defined in the previous subsection, various bolted faults (LG, LL, LLG, 3PH) were applied and the results were obtained by performing EMT time-domain simulations in DIgSILENT PowerFactory. These faults were studied assuming they 1) pre-existed prior to soft-starting the grid, 2) pre-existed prior to hard-starting the microgrid, and 3) occurred spontaneously after the grid has reached normal operating island state with all loads re-energized and supplied. Additionally, to understand the effect of resistive faults on the adaptive protection logic, LG faults on phase A with a fault resistance of 10ohms were also simulated and included in the test plan.

The performance of the adaptive protection scheme in response to motor starting current was examined for induction motors with sizes ranging in rating from 500kW to 2500kW in increments of 500kW. Similarly, for the transformer energization scenario, three different ratings of the transformer were considered: 500kVA, 1500kVA, and 2500kVA. Figure 3 depicts the voltage and current profile of a 1500kW motor starting scenario. Similarly, Figure 4 depicts the voltage and current profile of a 1500kVA transformer energization scenario.

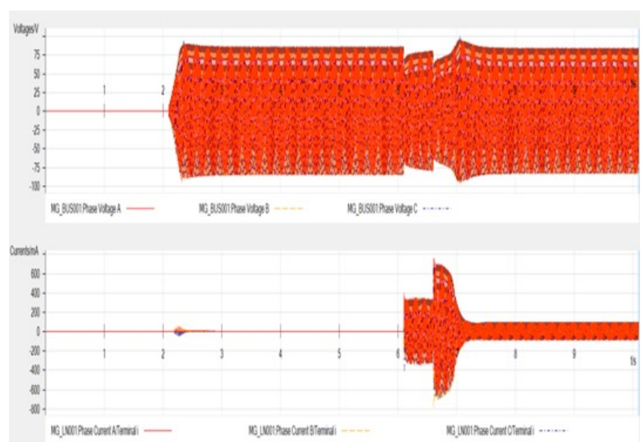

Figure 3. Three-Phase Voltage (top) and Current (bottom) waveforms for a 1500kW induction motor start

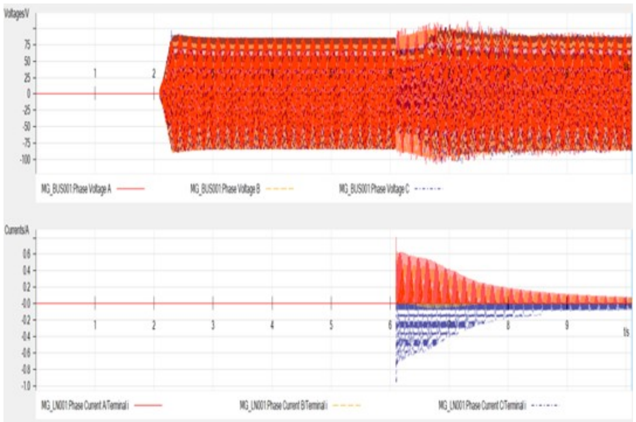

Figure 4. Three-Phase voltage (top) and current (bottom) waveforms for a 1500kVA transformer energization

Once the total number of cases to be run was defined, results (three-phase voltages and currents) from the simulations performed in DIgSILENT PowerFactory were exported as Common format for Transient Data Exchange (COMTRADE) files. These files were used to create test plan documents for playback to the protection relay with the programmed logic under test and the relay behavior was evaluated against set criteria in terms of trip time.

D. Test Results

Once the appropriate scenarios as discussed in the previous section along with their associated test plan documents were created, the final hardware test bench was set up using a three-phase test set to provide the three-phase secondary voltage and current signals to be fed to the relay. Figure 5 illustrates the information flow diagram of the test bench HIL setup used for testing the adaptive protection logic scheme. Connections for a trip and block contacts from the relay to the binary inputs of the test set enabled precise relay trip or block times to be included in the relay test report.

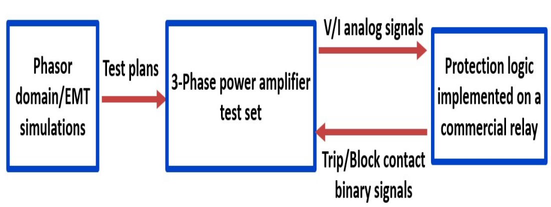

Figure 5. Information flow diagram of the HIL setup.

Figure 6 is a snapshot of the test plan document as well the final results obtained after running the tests. It was observed that the adaptive protection logic correctly tripped the relay for balanced and unbalanced faults (both bolted and resistive faults) during steady-state islanded, hard start, and soft start scenarios. The adaptive protection logic was also able to identify transformer inrush conditions and did not trip the relay even for the energization of the 2500kVA transformer, thus proving the robustness of the scheme.

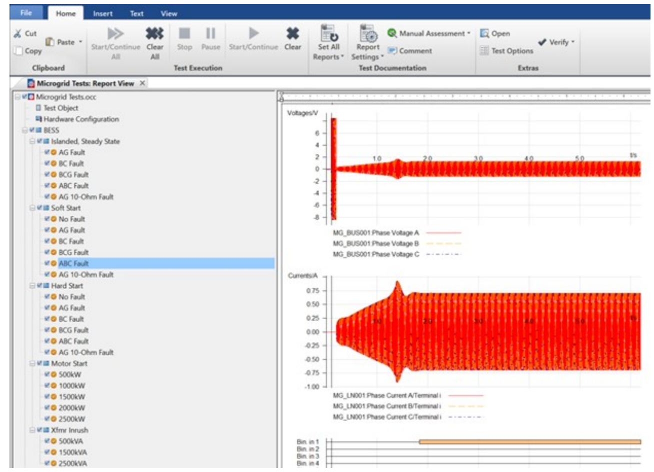

Figure 6. Snippet of test results for voltage-controlled overcurrent based adaptive protection Scheme.

During the motor start scenarios, it was observed that the adaptive protection scheme was able to perform as expected and did not mis-operate while starting motors rated up to 2000kW. It was only during the startup of a very large motor (2500kW in this case) that a trip signal was generated by the relay. Figure 7 depicts the voltage and current profile in this case. The "Bin in 1" signal refers to the TRIP contact status obtained from the relay. It can be seen that during the startup of such a large motor, the voltage dip is significant enough to trigger the undervoltage element in the relay which in turn frees the overcurrent element to operate due to the high motor starting current. Operating a single 2500kW motor in a microgrid with a single 3000kW BESS is considered an unlikely scenario, but in such exceptional cases, the undervoltage pickup element threshold or time-delay can be adjusted to coordinate with the motor starting current characteristics.

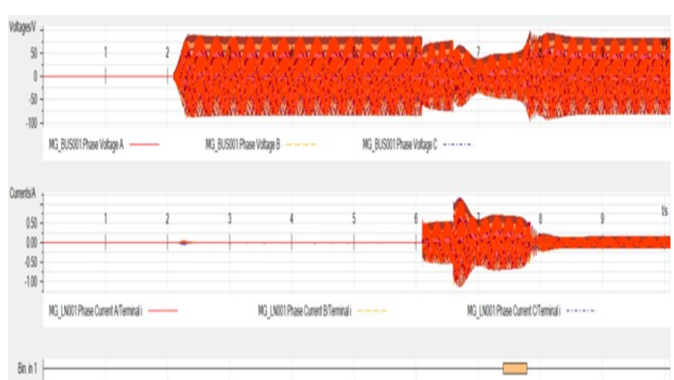

Figure 7. Three-Phase voltage (top) and current (bottom) profile during 2500kW induction motor start.

V. HIL TESTING, COMMISSIONING, AND DEPLOYMENT

A. Network model

The microgrid adaptive protection scheme was tested for a utility feeder that can be operated as a microgrid. The electrical boundary of the microgrid includes the area downstream of an Islanding Recloser that covers the feeder backbone and several three-phase and single-phase branches (laterals). The microgrid utilizes two Battery Energy Storage Systems (BESS) units for supplying customer loads under islanded mode. The BESS units are connected to the microgrid feeder at the Point of Common Coupling (PCC) through a recloser, which is also referred to as the PCC Recloser (see Figure 8). The microgrid is interfaced with the main grid at the Point of Interconnection (POI) via the Island Recloser.

The microgrid consists of two voltage levels, i.e., 34.5kV and 12.47kV. A simplified Single-Line Diagram (SLD) of the microgrid is shown in Figure 8, which includes the following:

- Feeder recloser: A recloser on the 12.47kV side of the microgrid feeder
- Islanding recloser and PCC recloser, located at the Medium-Voltage (MV) side (34.5 kV)
- Single-phase voltage regulators (one per phase) located downstream of the PCC recloser and upstream from the feeder recloser.
- Two Battery Energy Storage Systems (BESS) (2.2 MW each)
- An Intertie switch for connecting the BESS units
- Interconnection transformers for BESS inverters
- 1.5MVA grounding transformer (with 10-second short-circuit capacity) installed at the BESS switchgear

The maximum load on the microgrid is about 2MW, while the minimum load is about 350kW.

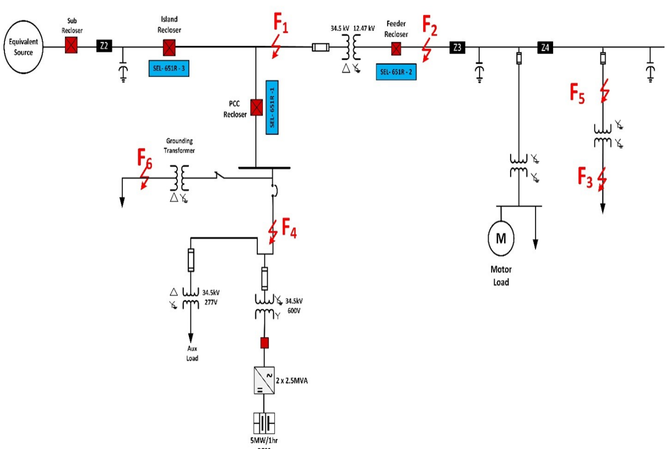

Figure 8. Simplified single-line diagram of the Microgrid.

B. *EMT simulations*

An Electromagnetic Transient (EMT) model of the microgrid was first simulated in the PSCAD/EMTDC software tool. Once the model was validated, the adaptive protection scheme was programmed in the relays and fault simulations were performed to determine the appropriate operation of the scheme. A total of 6 fault locations were considered (refer to Figure 8 and Table III). Multiple fault scenarios were simulated under both grid-connected and islanded modes of operation. In addition to the fault scenarios, other abnormal transient conditions like motor starting, and loss of one BESS unit were also simulated.

TABLE III. FAULT LOCATION DESCRIPTION

Faults	Description
F_1	Faults at the high side of the step-up transformer
F_2	Close fault downstream of feeder recloser
F_3	Far fault downstream of the feeder recloser (customer side)
F_4	Fault at the PCC (high side of the BESS transformer)
F_5	Far fault downstream of the feeder recloser (utility side)
F_6	Fault on the low side of the grounding transformer

Simulation results showed that under grid connected mode, the traditional protection elements provided appropriate protection during faults and operated much quicker than the adaptive protection scheme elements. However, under the islanded mode, the fault currents were much lower than the overcurrent pickups for these elements. In these cases, the adaptive protection scheme provided the necessary coverage.

One fault location that proved a challenge both for the existing protection scheme and the adaptive protection scheme is location F_3. The impedance of the transformer is so high that faults at this location cannot be detected by the protection elements in the reclosers. For faults at this location, the transformer protection device will need to be relied on to clear the fault. Similarly, faults at location F_6 under islanded mode will not be detected by the reclosers programmed with the adaptive protection scheme. The grounding transformer's in-built protection devices would have to clear these faults.

C. *Closed Loop HIL (CHIL) Test Results*

Once the EMT simulations had been completed and protection setpoints for the various relays calculated, but before programming the actual relays in the field and putting the scheme in-service, closed loop hardware in the loop testing was performed on the scheme. While this step is not always necessary, in this case, it was included to fully understand the behavior of the relays that would be programmed with this scheme in the field. A Real-Time Digital Simulator (RTDS) was used for this purpose.

A detailed model of the microgrid was constructed in the RSCAD software tool. The RSCAD model was compared with the EMT model of the system, developed in the PSCAD/EMTDC software tool, to ensure accuracy. The objective was to ensure these two models match each other from the power-flow and short-circuit perspectives. The model validation studies showed that the RSCAD model of the microgrid feeder (i.e., the backbone of the microgrid) provides an accurate representation of the feeder.

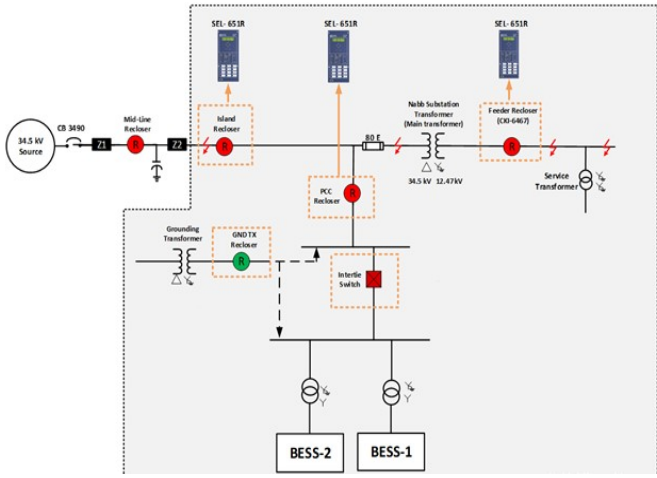

Figure 9. Hardware in the Loop RTDS Setup.

More than 96 test cases were performed using the RTDS HIL testbed, and the test results were analyzed to evaluate the performance of the proposed adaptive protection scheme. The parameters considered in the test case selection included: Microgrid operating mode, Fault type, Fault duration, Fault location, Fault impedance; BESS Charge/Discharge mode, and Transient switching scenarios.

The performance evaluation of the adaptive protection scheme resulted in three potential outcomes as follows:

Pass

- The expected protection element(s) picks up.
- The closest relay to the fault (main relay) trips for a fault in its immediate tripping zone, or
- The backup relay waits to initiate a trip with some delay when the fault is not in its tripping zone.

Conditional Pass

- Unexpected/Undesired protection element picks up but the main relay trips for faults in its immediate tripping zone, or
- Unexpected/Undesired protection element picks up, but the backup relay waits to initiate a trip with some delay when the fault is not in its immediate tripping zone.
- The relay trips for faults in its tripping zone, but with longer operating times than expected.

Fail

- The relay does not detect a fault in its immediate zone (or does not trip for a fault in its immediate zone).
- The relay trips before other relays where the fault is not in its immediate tripping zone.

Case 1

In Case 1, the microgrid operates in the grid-connected mode, and a low-impedance three-phase-to-ground fault (3LG) happens at the end of the feeder downstream of the service transformer (i.e., Location F_3 in Figure 8). In this case, both BESS units are operating under maximum discharge level (1.375 MW per BESS). It was seen that the fault at Location F_3 cannot be detected by the feeder recloser (i.e., the closest protective device) (See Figure 10). The reason is that the fault current (~140A) for a fault downstream of the service transformer is not large enough to trigger the inverse time overcurrent (51) elements. Also, due to the very small voltage drop (less than 0.05pu), the voltage-supervised 50P elements were not triggered. Therefore, the protection system cannot detect and isolate the fault. However, this is believed to be an existing problem in the system (caused by the small rating, and large impedance of the service transformer).

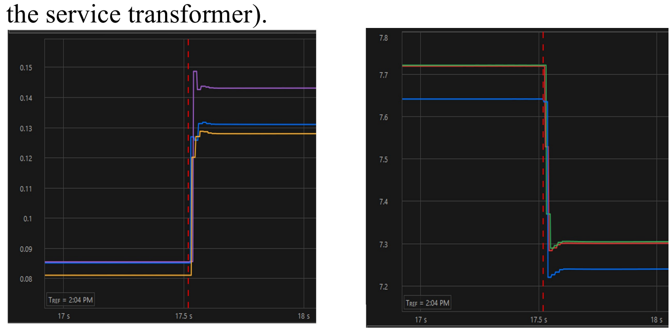

Figure 10. Current (in kA, left) and Voltage (in kV, right) measured by Feeder Recloser for F_3 fault in grid-connected mode

Case 2

In Case 2, the microgrid operates in islanded mode, and a high-impedance (10Ω) three-phase-to-ground fault (3LG) is simulated at the end of the feeder upstream of the service transformer (i.e., Location F_5 in Figure 8). For this fault case, though the fault current (~ 0.27 kA) which is only provided by the BESS units is small, it causes the definite-time element of the feeder recloser (i.e., 50P) to trip in 0.61s after the fault (See Figure 11). This fault case can be considered as one of the worst-case scenarios for the protection system; however, the adaptive protection scheme can detect the fault with the sensitive but voltage-supervised protection elements.

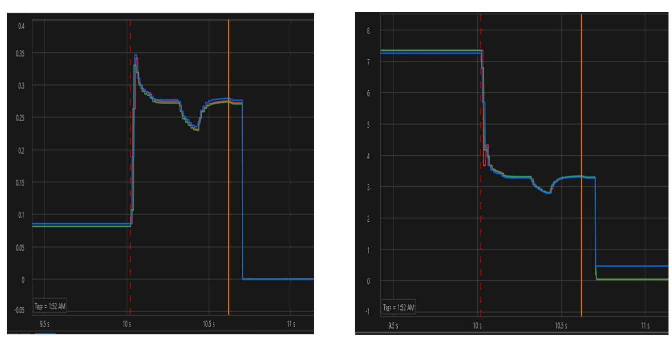

Figure 11. Current (in kA, left) and Voltage (in kV, right) measured by Feeder Recloser for F_5 fault in islanded mode

VI. CONCLUSIONS AND FUTURE WORK

The simulation study results show that the adaptive protection scheme using voltage-controlled overcurrent elements can appropriately detect and isolate a majority of fault scenarios within the microgrid if the protection settings are selected properly. Therefore, it is essential to perform the required system studies prior to the adaptive protection scheme deployment and ensure accurate selection/calculation of the settings for the microgrid under study. This is particularly important because the proposed adaptive protection scheme can be used in the absence of communications to the microgrid controller.

In some cases where the fault is located downstream of service transformers or toward the end of the feeder, the protection system fails to detect the fault. This, however, is a problem that may happen in the existing system. Since the customer has their own protection system (not included in this study), it can be considered that customer-side faults can be detected by the customer's protection system(s). It should also be noted that since the proposed adaptive protection scheme is designed to work under both microgrid operating modes, the relay operating times are larger in islanded mode. As such, arc flash studies should be performed to ensure safety for any live work.

Next steps involve obtaining and analyzing field data from this microgrid to observe the performance of the adaptive protection scheme and implementing this scheme at other sites to obtain additional insight into the scheme's performance and efficacy. To get further confidence in this scheme, the authors are working with utilities that currently have microgrids within their service territories to obtain COMTRADE files from various events that may have occurred within their microgrids to play these events back to a relay programmed with the proposed adaptive protection scheme in the laboratory and observe the scheme's performance to these events.

Appendix 1 – Relay Specific Implementation of Tripping Logic

A SEL-451 relay was used for laboratory testing of the adaptive protection tripping logic in the pre-deployment stage. The logic was implemented with the combined usage of the 27 (undervoltage) and 51 (time overcurrent) elements in the SEL-451 relay. The relay was configured to enable three per-phase undervoltage elements (27) when the adaptive protection scheme was enabled. The undervoltage elements were supervised by the absence of relay and measurement alarms. Figure 12 depicts the settings for the phase A undervoltage element.

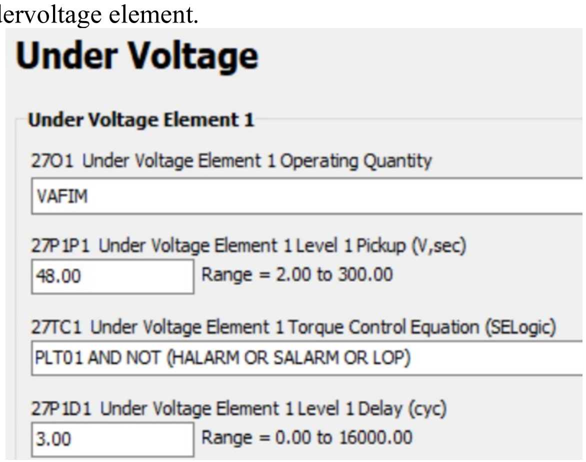

Figure 12. Undervoltage Element Configuration Settings for Phase A

The undervoltage pickup level was set at 48 V (around 80% of the nominal secondary voltage) with a pickup delay of 3 cycles. The undervoltage element is activated only when the adaptive protection scheme is enabled (PLT01) and there are no relay alarms (HALARM or SALARM) and a loss of VT fuse condition does not exist (LOP). Different manufacturers have different implementations for the logic that determines VT fuse failure. In this case, SEL's built-in logic was relied on to make this determination.

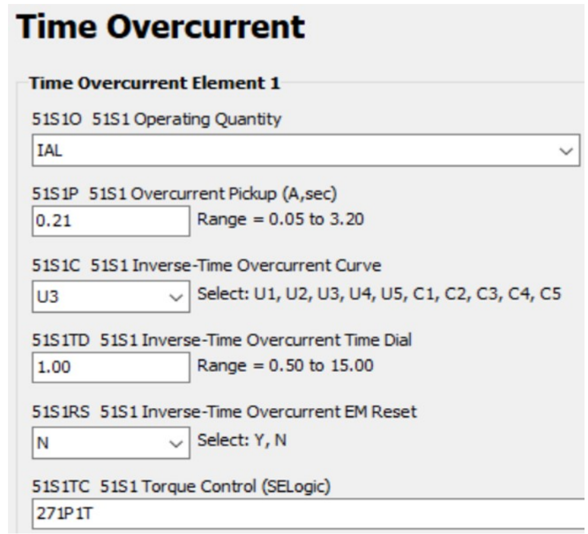

Figure 13. Time Overcurrent Element Configuration Settings for Phase A

Similarly, Figure 13 depicts the time overcurrent element settings for phase A where the overcurrent pickup element (51) was configured to be enabled once the undervoltage element has timed out (271P1T). In this case, a pickup value of 0.21A secondary (70A primary) was chosen for the 51 element. The time overcurrent element follows a U3 curve set at a time dial setting of 1.0. Similar elements were programmed for phases B and C.

Acknowledgment

The material presented in this paper is based upon work supported by the U.S. Department of Energy's Office of Energy Efficiency and Renewable Energy (EERE) under the Solar Energy Technologies Office Award Number DE-EE0009019. The authors gratefully acknowledge the contributions of all the associated members of the PV-MOD project.

References

[1] K. Maki, S. Repo and P. Jarventausta, "Blinding of Feeder Protection Caused by Distributed Generation in Distribution Networks," in WSEAS Int. Conf on Power Systems and Electromagnetic Compatibility, Corfu, Greece, 2005.
[2] T. K. Barik and V. A. Centeno, "Decentralized Multi-setting Adaptive Distribution Protection Scheme for Directional Overcurrent Relays", in 2020 IEEE Kansas Power and Energy Conference (KPEC), Manhattan, KS, USA, 2020, pp. 1-6.
[3] "Adaptive Protection: Adaptive Protection and Validated MODels to Enable Deployment of High Penetrations of Solar PV (PV-MOD)", EPRI, Palo Alto, CA: 2023. Milestone 2.9.2 Report for DOE.
[4] T. K. Barik, K. M. Phelps, J. J. Petti and F. Velez-Cedeno, "A Multi-principle Passive Islanding Detection Technique for Power Distribution

Systems”, in 2019 IEEE Power & Energy Society General Meeting (PESGM), Atlanta, GA, USA, 2019, pp. 1-5.
[5] A. Hooshyar and R. Iravani, "Microgrid Protection," in Proceedings of the IEEE, vol. 105, no. 7, pp. 1332-1353, July 2017, doi: 10.1109/JPROC.2017.2669342.
[6] H. J. Laaksonen, "Protection Principles for Future Microgrids," in IEEE Transactions on Power Electronics, vol. 25, no. 12, pp. 2910-2918, Dec. 2010, doi: 10.1109/TPEL.2010.2066990.
[7] E. Sortomme, G. J. Mapes, B. A. Foster and S. S. Venkata, "Fault analysis and protection of a microgrid," 2008 40th North American Power Symposium, Calgary, AB, Canada, 2008, pp. 1-6, doi: 10.1109/NAPS.2008.5307360.
[8] J. Shiles et al., "Microgrid protection: An overview of protection strategies in North American microgrid projects," 2017 IEEE Power & Energy Society General Meeting, Chicago, IL, USA, 2017, pp. 1-5, doi: 10.1109/PESGM.2017.8274519.
[9] T. K. Barik and V. A. Centeno, “Dynamic Prioritization of Critical Loads for Sustaining Power Distribution Systems upon Islanding”, in *2020 IEEE Power & Energy Society Innovative Smart Grid Technologies Conference (ISGT)*, Washington, DC, USA, 2020, pp. 1-5.
[10] "IEEE Standard for the Specification of Microgrid Controllers," in IEEE Std 2030.7-2017 , vol., no., pp.1-43, 23 April 2018, doi: 10.1109/IEEESTD.2018.8340204.
[11] Barik, T.K., 2021. Modern adaptive protection and control techniques for enhancing distribution grid resiliency (Doctoral dissertation, Virginia Tech).